Oceanologia, uncorrected, in press
Polish Academy of Sciences
Institute of Oceanology

https://doi.org/10.5697/...

Geohazards and coastal dynamic: Geo-engineering assessment of the southern Iraqi shore (Ras al-Bisha zone)

Hiba Ahmed Mahdi [1], Wisam R. Muttashar [2,*], Raid Aziz Mahmood [1]

Abstract

The coastal zone of Ras al-Bisha, located between the mouth of the Shatt al-Arab River and the eastern breakwater of the Grand Faw Port, exhibits complex interactions of tidal forces, sediment transport, and anthropogenic modifications. This study develops an engineering geological framework to assess sediment stability and geohazard potential under semi-diurnal tidal conditions. Field measurements, including in situ vane shear tests at 41 stations, were used to determine undrained shear strength and derive critical shear stress for surface sediments. Hydrological data provided ebb and flood current velocities and water levels. A dual factor of safety (FS) approach was introduced to evaluate sediment stability separately for ebb and flood tides, producing spatially explicit maps of stable ($FS > 1.5$), critical ($1.0 \leq FS \leq 1.5$), and unstable ($FS < 1.0$) zones. The results reveal an inland-to-seaward gradient in sediment strength and resistance, with very soft to soft sediments dominating the nearshore environment. Flood tides generate higher applied shear stresses than ebb tides, leading to expanded unstable zones along the shoreline front. Erosion rate analyses confirm greater sediment displacement during flood conditions, while ebb tides partially mitigate instability. The dual-FS hazard maps offer a refined way for prioritizing monitoring and mitigation efforts, directly informing coastal management and infrastructure planning in estuarine settings affected by bidirectional tidal dynamics.

Keywords

Iraqi shore; Geohazard mapping; Ebb and flood tide dynamics; Sediment stability; Coastal erosion risk

[1] *Geology Department, College of Sciences, University of Basrah, Basra, Iraq*
[2] *Marine Science Center, University of Basrah, Basra, Iraq*
***Correspondence**: wisam.muttashar@uobasrah.edu.iq (W.R. Muttashar)

Received: 8 July 2025; **revised:** 10 October 2025; **accepted**: 8 December 2025

List of abbreviations and acronyms

ASTM American Society for Testing and Materials

D2573 ASTM Standard D2573 (field vane shear test)

D422 ASTM Standard D422 (particle-size analysis of soils)

D4318 ASTM Standard D4318 (liquid/plastic limit tests)

FS factor of safety

FS_{ebb} Factor of safety under ebb-tide conditions

FS_{flood} Factor of safety under flood-tide conditions

GFP Grand Faw Port

GCPI General Company for Ports of Iraq

MSC Marine Science Centre

List of symbols

γ_w Unit weight of water (kN m^{-3})

d Water height above midpoint (m)

S Slope of the energy grade line (dimensionless)

τ_a Applied fluid shear stress (Pa)

$\tau_{a\,Ebb}$ Applied fluid shear stress during ebb tide (Pa)

$\tau_{a\,Flood}$ Applied fluid shear stress during flood tide (Pa)

τ_c Critical shear stress of sediment (Pa)

S_u Undrained shear strength of sediment (kPa)

β Dimensionless constant (2.6×10^{-4})

1. Introduction

The stability of coastal environments is shaped by a complex interplay of natural forces and human interventions. Global studies of sediment stability and geohazards have established that shoreline erosion and changes in sediment dynamics present substantial threats to infrastructure and ecosystems. Researchers have used approaches such as numerical and empirical modeling, remote sensing, and risk assessment frameworks to quantify sediment movement, monitor coastal change, and support adaptation (Liu et al., 2023; Sun et al., 2025). Sophisticated methods integrating field measurements, modeling, and remote sensing have elucidated mechanisms behind erosion, land subsidence, liquefaction, and slope failures, with particular attention to environments at risk of flooding and engineering hazards (van Rijn, 2016). Hashemi et al. (2014) implemented a hazard mapping framework integrating geological, sedimentological, and geotechnical data, relying on boreholes and dynamic cone penetrometer tests across a deltaic setting. They identified unstable Holocene sediments most prone to liquefaction, erosion, and subsidence, enabling zonation for risk management and future urban planning. However, a consistent finding among global studies is that tailored site-specific investigations remain indispensable for effective management, given the unique geological, hydrodynamic, and socio-economic factors that shape coastal sediment stability and hazard profiles (van Rijn, 2016).

In the study region, previous studies have examined shoreline instability, highlighting the large reduction in sediment supply due to upstream water management projects. Remote-sensing analyses have captured significant shoreline change in the northern Arabian/Persian Gulf and have shown both retreat and episodic progradation, especially under tidal and wave influences (Al-Aesawi et al., 2020; Aladwani, 2022; Al-Fartusi, 2023). The southern Iraqi coast – specifically the Ras al-Bisha region between the mouth of the Shatt al-Arab River and the eastern breakwater of the Grand Faw Port (Figure 1), presents unique sedimentary and hydrodynamic characteristics that warrant a detailed geotechnical and hazard assessment (Mahdi et al., 2025). This region faces energetic tidal fluctuations, sediment transport dynamics, and anthropogenic modifications, all contributing to significant erosion, deposition rates, and coastal morphology changes (Albadran and Albadran, 1993; Albadran et al., 2002; Al-Aesawi et al., 2020; Muttashar et al., 2024). Muttashar et al. (2024) tracked coastline changes using historical bathymetric charts and the Digital Shoreline Analysis System (DSAS), reporting an average shoreline retreat of 3.48 m year^{-1} for the Iraqi side and linking these changes to sediment composition and physical controls identified from a few geotechnical measurements taken from the literature, such as shear strength of the sediment. Mahdi et al. (2025), in their comprehensive review, emphasized the critical need to focus on the field mechanical properties of sediments, noting that research in this specific aspect remains limited. Such

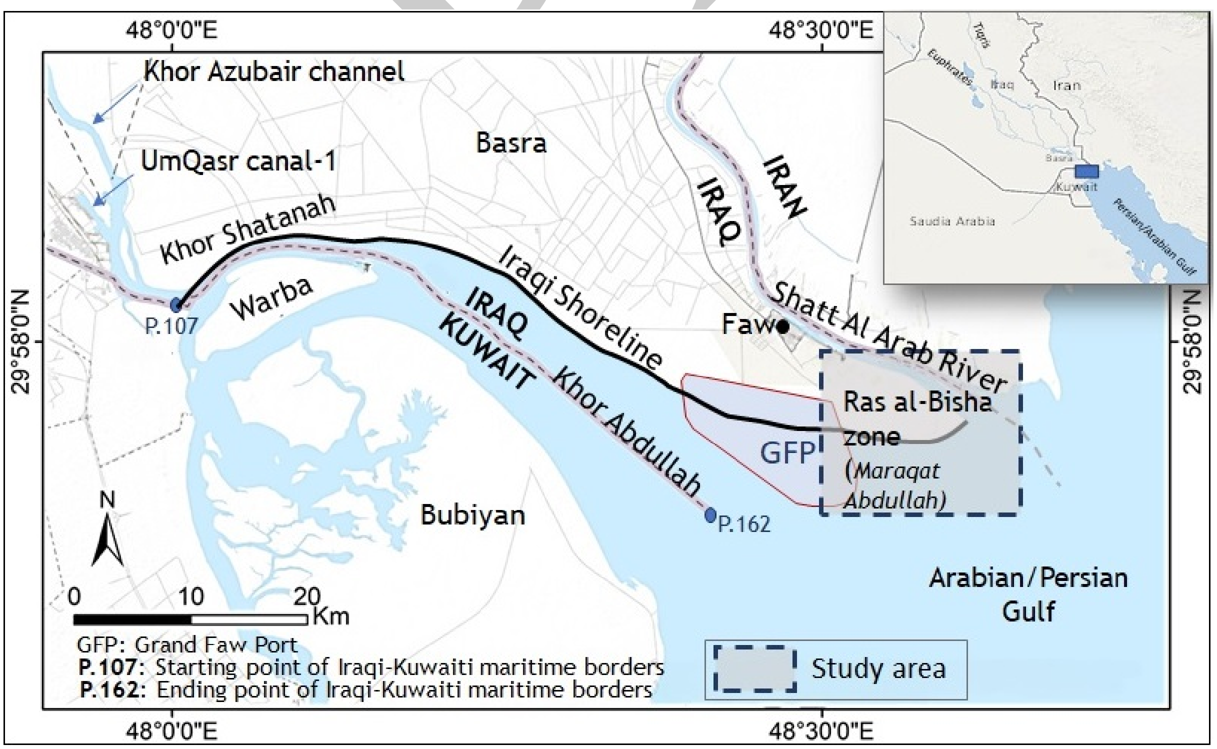

Figure 1. Location map of the study area.

studies are essential for evaluating sedimentation hazards and accurately determining erosion rates. Assessing sedimentation rates typically requires factoring in tidal current dynamics and measurements of the sediment shear strength (Muttashar et al., 2025). In their research, the measurements of critical shear stress and safety factors for both ebb and flood tide conditions were conducted to quantify erosion rates occurring during these tidal events.

Previous research often focuses separately on either historical shoreline changes or specific sediment characteristics, without integrating these findings into robust hazard assessment models for engineering and management purposes. Connections between coastal engineering activities, changing hydrodynamic conditions, and their combined influence on erosion are only starting to be explored (Muttashar et al., 2024; Mahdi et al., 2025). Bridging these gaps is essential for improving coastal risk monitoring and ensuring the sustainable management of Iraq's increasingly vulnerable shorelines.

This study seeks to develop engineering geological hazard maps and to conduct a detailed assessment of erosion rates, with a particular emphasis on the factor of safety, a critical measure for understanding sediment stability under dynamic marine influences. This approach qantifies the ratio between the critical shear stress of sediment and the critical shear stress of water, providing independent evaluations for ebb tide conditions and flood tide conditions. The significance of this approach is considering the varying shear velocity characteristics of seawater at ebb and flood tides, where a dual factor of safety will be introduced. This enhances hazard mapping and supports precise coastal risk assessment in dynamic marine situations.

2. Theoretical background

The fluvial and coastal processes governing sediment stability are inherently tied to the interactions between hydraulic forces and geotechnical properties of the sediments (Muttashar et al., 2025). The fundamental parameters driving erosion, deposition, and sediment transport include applied fluid shear stress (τ_a) and critical shear stress (τ_c) for sediment, which dictate sediment detachment and transport mechanisms. The semi-diurnal tidal nature of the Ras al-Bisha region introduces dual hydraulic behaviors, requiring an advanced framework for evaluating sediment stability under both ebb and flood tide conditions.

The hydrodynamic regime in Ras al-Bisha is categorized as a semi-diurnal tidal system (Lafta, 2023), meaning that ebb and flood tide currents exert alternating influences on sediment stability (Muttashar et al., 2025). Unlike traditional coastal stability analyses, where a single factor of safety (FS) is used, this study introduces a dual FS approach to account for dynamic bidirectional shear stress conditions: (FS_{ebb}) considers the shear stress exerted by ebb tide currents.

FS_{flood} considers the shear stress exerted by flood tide currents.

The fluvial process can be presented using the average applied fluid shear stress, τ_a, as a parameter showing the hydraulic river characteristics:

$$\tau_a = \gamma_w \, d S \tag{1}$$

where γ_w is the unit weight of water (kN m^{-3}), d is water height above midpoint (m), and S is slope of the energy grade line, approximated by the channel slope. This fluid shear stress (τ_a) is a crucial indicator of the erosion process by comparing the fluid shear stress with the critical shear stress of the riverbank material (τ_c). The critical shear stress expresses the strength of the sediment consisting of the riverbanks or beds.

Soil properties seem to be the crucial factor in evaluating the bank stability against the hydraulic factors of the river. Léonard and Richard (2004) developed a significant relationship between τ_c and undrained shear strength (S_u), with a high coefficient of correlation ($R^2 = 0.93$), as described in Equation (2).

$$\tau_c = \beta(S_u) \tag{2}$$

β is a dimensionless constant equal to (2.6×10^{-4}), resulting from experimental tests. In this study, undrained shear strength measured through the geotechnical tests of the selected sites was used to estimate the critical shear stress of the surficial sediment layer (τ_c), in which erosion of surficial sediment layer takes place if τ_a exceeds τ_c.

Both τ_a and τ_c are well correlated to the rate of erosion of the sediments, and the erosion rate (ε) can be estimated as a function of τ_c. Thus, erosion can be expressed through the factor of safety (FS) (Muttashar et al., 2025):

$$\varepsilon = \mathrm{FS} = \frac{\tau_c}{\tau_a} \tag{3}$$

The study area has two hydraulic behaviors (flood and ebb tides) daily at approximately 6 hours for each behavior (Lafta, 2021). As a result, the flood and ebb currents act at two hydraulic statuses in terms of velocity direction and magnitude, acting uniformly. In the flood tide status, the direction of the flood currents is opposite to the ebb ones, causing the currents' direction to change water speed (u). The two cases of the tidal river should be considered when the effect of the fluid shear stress on the grains detaching is analyzed. Specifically, this study evaluates whether the tidal flood and ebb currents, noted as $\tau_{a\,Flood}$ and $\tau_{a\,Ebb}$, respectively, exceed or fall below than critical shear stress, τ_c. Therefore, this research examines this two-fluid shear stresses.

Thus, Equation (1) could be expressed as $\tau_{a\,Ebb} = +\gamma_w d S$ at tidal ebb conditions, and $\tau_{a\,Flood} = -\gamma_w d S$ at tidal flood conditions.

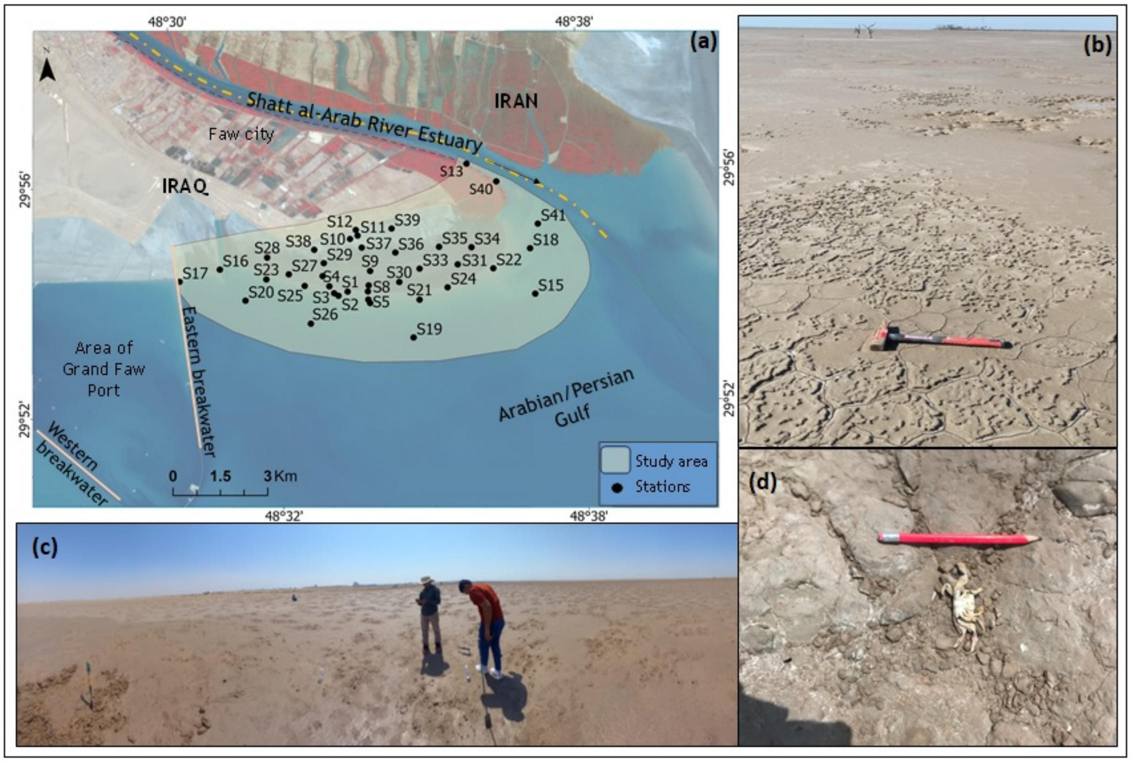

Figure 2. The measurement sites, accompanied by photographs illustrating the muddy sediment characteristics within the study area.

After determining τ_c and checking if $\tau_a \geq \tau_c$, sediment erosion exists. To test the required parameters to evaluate the hazard levels of the coastal sediment instability, hydrological and geotechnical measurements were performed.

3. Material and methods

3.1 Site description

The studied region, specifically the shore area, the Ras al-Bisha zone between the Shatt al-Arab River mouth and the eastern breakwater of the Grand Faw Port, as shown in Figure 1, exhibits distinct sedimentary and dynamic hydrodynamic conditions. It is characterized by complex interactions of riverine and estuarine processes (Muttashar et al., 2021; Alfaris et al., 2024). The study area features fine-grained soils with elevated silt and clay content (Alkhafaji et al., 2023; Al-Asadi et al., 2023). The land progressively declines toward the Gulf in the southern region of the sedimentary plain, beginning with the coastal marshes in the north and reaching the lowest elevation of the islands in the southernmost area (Albadran, 2004).

The study region comprises a tidal flat strip that stretches from the eastern bank of the Shatt al-Arab River to the entrance of the Khor al-Zubair channel, approximately 36 nautical miles in length, as illustrated in Figure 1. The region is defined as a shallow zone exhibiting an arid climate during the summer and a humid climate in the winter (Darmoian and Lindqvist, 1988). The sedimentary processes on the Iraqi coast are affected by the sediments provided by the Shatt al-Arab River and Khor Abdullah waterway, as well as tidal and coastal currents (Albadran and Albadran, 1993).

The region shows instability attributed to the velocity and dynamics of the waves, as well as the climatic conditions influencing the tidal currents (Al-Amery and Al-Saad, 2002). The tide conditions exhibit a mixed tidal regime that is predominantly semi-diurnal, featuring two unequal high and low tides most days (Lafta, 2022). Tidal ranges vary significantly, from about 1 meter near Basra to as much as 3 meters at Faw and the river mouth, reaching approximately 3.7 meters during spring tides (Al-Fartusi, 2022), with strong tidal current velocities up to 1 m s^{-1} recorded near the river mouth. These tidal forces play a dominant role in shaping the hydrodynamic and environmental conditions along the Iraqi coast and Shatt al-Arab Estuary.

The earlier study by Mahdi et al. (2025) identifies the construction of the Grand Faw Port (GFP) as a pivotal intervention that has introduced a new coastal configuration requiring further scientific investigation. This development has effectively divided the Iraqi shoreline into two morphologically distinct segments: the eastern shoreline, which stretches from the western bank of the Shatt al-Arab River to the eastern breakwater of the GFP, and the western shoreline, which extends over 34 km from the port's western breakwater to Khor Shatanah at point 107 (see Figure 1). The present study concentrates on the eastern segment, particularly the Ras al-Bisha zone, due to its pronounced geomorphological dynamics and evident instability resulting from ongoing erosional and depositional processes.

Figure 2 illustrates the spatial extent of the study area and the distribution of measurement sites (S1 to S41) located between the Shatt al-Arab River estuary and eastern breakwater of GFP. The study area, as presented in field photographs b, c, and d, brings about the natural surficial conditions of the tidal flat sedimentary environment investigated.

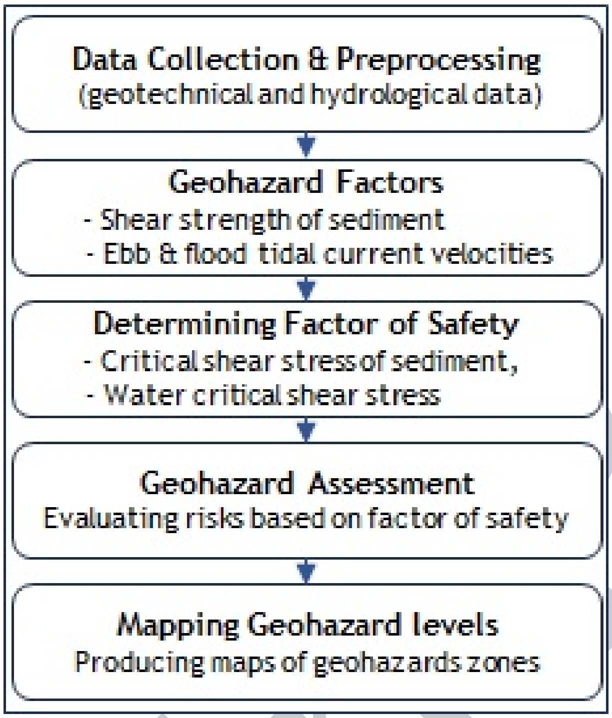

Figure 3. Key steps of the research methodology.

The flowchart (Figure 3) illustrates the key steps in the methodology of this research, providing a clear overview of the evaluation of sediment stability for the development of geo-engineering hazard maps for the southern part of the Iraqi coast, specifically the Ras al-Bisha zone.

The flow chart presents a systematic approach for evaluating and delineating geohazards, consisting of five consecutive steps. The process commences with Data Collection and Preprocessing, involving the acquisition and preparation of critical geotechnical and hydrological data for subsequent analysis. The subsequent phase, Geohazard Factors, emphasizes the assessment of critical parameters including sediment shear strength and tidal current velocities under ebb and flood conditions. The next step involves determining the factor of safety, which includes calculating the critical shear stress of sediments alongside the corresponding water-induced shear stress to evaluate stability. The Geohazard Assessment phase employs these calculations to assess potential risks and pinpoint vulnerable areas. The Mapping Geohazard Levels step converts assessment results into spatially explicit maps, facilitating the visualization of hazard-prone areas.

3.2 Geotechnical measurements

The main purpose of the geotechnical data is to detect the critical shear stress (τ_c) dependent on the shear strength parameter of the sediment layer. To do so, in situ shear strength measurements were implemented.

3.2.1 Field shear strength measurements:

Forty-one sampling stations, designated S1 to S41 (see Figures 2 and 3 were established for the study. Thirteen of these stations were estimated by extrapolation from measurements from nearby sites and validated through satellite imagery color patterns, as certain areas were difficult to access. The field vane shear equipment was used, following the ASTM Standard (D 2573). It is an instrument consisting of a rod connected to an iron feather at one end and a torque arm at the other end. The feather is penetrated to the required depth, then the torque arm is rotated and the torque is calculated. The aim is to calculate the shear strength (S_u) of the soil on-site. This method, known as the vane shear test, was selected because it is particularly well-suited for soft, cohesive sediments, which are dominant in the study area. Such sediments often pose challenges for other geotechnical testing tools due to their low strength and high-water content, making the vane shear test a reliable and practical choice for obtaining accurate in-situ measurements in these conditions.

3.2.2 Classification tests

The particle-size and plasticity analysis of the eight soil samples were performed using the ASTM standard (D422 and D4318) to identify the soil types. taken from a depth of 10 cm to 1 meter, focusing on the first 20 cm representing the surface sediments of the area affected by marine processes. Table 1 shows typical sediment sample analysis of the study area.

Table 1. Typical sediment characteristics of the study area.

Characteristics	Value
Fine%	94%
Sand%	6%
Silt%	70%
Clay%	24%
PI	7%
LL	39%

3.3 Hydrological measurement

The hydrological parameters are essential to estimate the fluid shear stress (τ_a) at the selected sites and subsequently estimate the erosion rate at both (ebb and flood) tide conditions. Hydrological data were collected from hydrographic station near the breakwater at 29°50′2.24′′N, 48°28′45.27′′E, which was constructed by Daewoo Engineering & Construction Co., Ltd. at the western breakwater of Al-Faw port in the entrance of the Khor Abdullah waterway. An hourly record of the water level, currents directions and magnitudes for the entire month was used.

4. Results

4.1 Geotechnical consideration

4.1.1 Sediment shear strength

Across 41 sampling stations labeled S1 through S41 (Figures 2 and 3) the dataset exhibits notable spatial variability of sediment shear strength (S_u), measured in kilopascals (kPa). As illustrated in Table 2, the maximum shear strength was recorded at Station S10, reaching approximately 45 kPa, whereas the minimum value of about 5 kPa occurred near Station S16. Based on the trend, the average shear strength typically falls within the range of 20 to 25 kPa.

Table 2. Trend of sediment shear strength parameter.

Shear strength parameter	Value/Station
Minimum value	5 kPa at Station S16
Maximum value	45 kPa at Station S10
Average range	20–25 kPa (estimated)

Based on the Terzaghi et al. (1996) classification, the measured undrained shear strength (S_u) values across the stations can be categorized into distinct clay consistency classes. Stations exhibiting S_u values below 12 kPa fall into the 'very soft' clay category, indicating extremely weak and compressible sediments; this includes sites like S16. Values ranging from 12 to 25 kPa would be considered 'soft', while those between 25 and 50 kPa are classified as 'medium' consistency. The majority of the S_u values in the dataset lie within the very soft to medium range. This classification suggests that the sediment across the study area is generally weak to moderate level of shear strength.

Figure 4 shows typical profiles of field undrained shear strength measured to a depth of approximately 100 to 110 cm. This illustrates the behavior of S_u within the initial one meter indicating a low to very low shear strength of the soil. The S_u values typically decline with increasing depth, beginning at 20–30 kPa at 10 cm and decreasing to 8–10 kPa at 120 cm. The overall trend (dashed line) demonstrates a consistent and gradual decline in undrained shear strength as depth increases. The observed decline may indicate a weak layer or the impact of saturation lowering effective stress as a result of groundwater influence, implying uniform soil conditions.

Geographically, the general trend of undrained shear strength decreases from the land toward the sea. Figure 5 reveals this S_u trend at four sites indicating a decrease in S_u from the land (site# S10) toward the sea (site# S19), suggesting sediment becomes less resistant toward the sea.

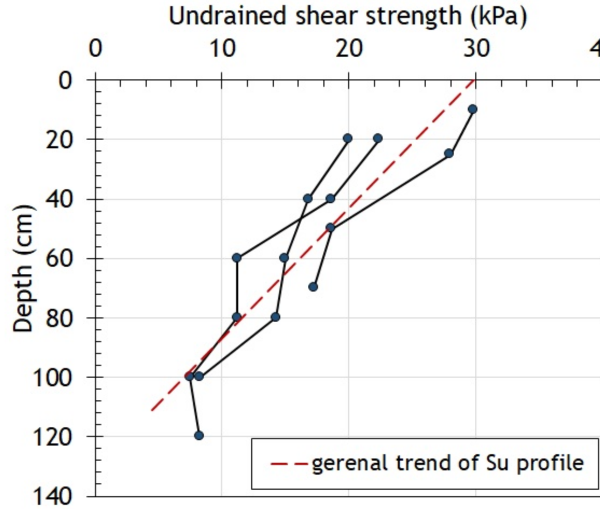

Figure 4. Typical undrained Van shear strength profiles showing ideal trend of S_u in the study area.

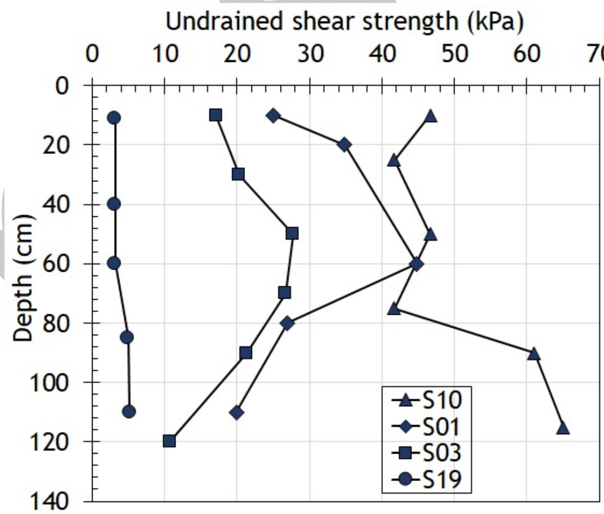

Figure 5. General undrained shear strength profiles at four sites indicating decrease in S_u from the land S10 toward the sea S19.

It is important to note that while a general decline in undrained shear strength (S_u) with depth is observed across many sites (Figure 4), this trend is not consistently evident at all locations, particularly at sites S19 and S10, as illustrated in Figure 5, which presents the horizontal (geographical) variation in S_u. At the seaward site S19, S_u values are extremely low (less than 10 kPa), making it difficult to discern a clear vertical trend within the first meter. This may be due to high saturation levels with insufficient effective stress of the surficial sediment layer. In contrast, site S10, situated further inland, shows no distinct S_u trend

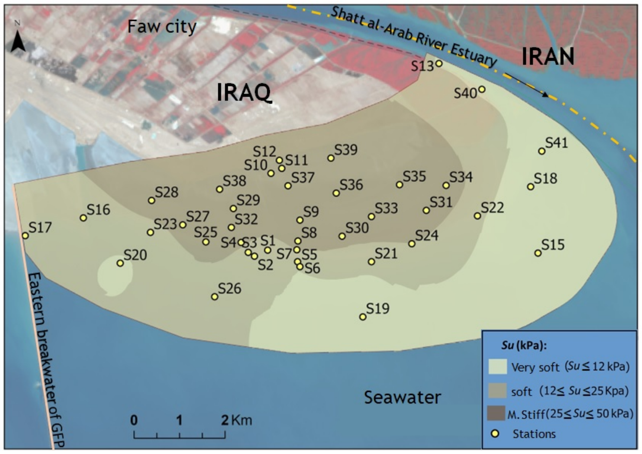

Figure 6. Distrubtion of shear strength (S_u) for sediment.

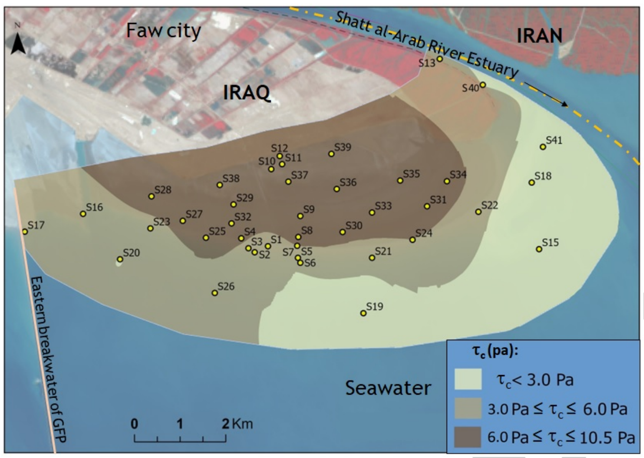

Figure 7. Spacial distrubtion of critical shear stress (τ_c) for sediment.

in the upper 80 cm, but an increase in strength is observed below that depth. This pattern aligns with typical inland sediment behavior, where increasing effective stress due to compaction enhances shear strength with depth.

4.1.2 Shear strength and critical shear stress of the coastal sediments

Figure 6 reveals the spatial variation in the undrained shear strength of sediment (S_u) across the study area. In Figure 6, the sediment is grouped into three consistency categories: very soft, soft, and medium stiff. The inland regions, particularly those closer to the upper boundary of the map, are dominated by medium-stiff sediments, indicating areas with consolidated, compacted clays. Moving seaward, a clear spatial gradient emerges: sediment shear strength gradually decreases toward the seaside, where soft and very soft sediments become more prevalent, which implies recent accumulation, higher water content, and lower stability. These nearshore zones are characterized by fine-grained, water-saturated, and loosely packed sediments, traits commonly associated with active deposition zones and tidal influence.

Figure 7 presents the spatial variation of the critical shear stress (τ_c) of surface sediments across the study area, with values expressed in pascals (Pa). Critical shear stress represents the minimum force required to initiate sediment movement, making it a key parameter in evaluating sediment stability and erosion potential. The legend classifies τ_c into three categories: very low resistance (< 3.0 Pa), low resistance (3.0–6.0 Pa), and intermediate resistance (6.0–10.5 Pa), allowing for a clear visual distinction of sediment strength across the region.

A distinct spatial trend is evident in the distribution of τ_c values. Toward the inland areas, particularly near the river's creeks and away from direct marine influence, sediments generally exhibit the highest critical shear stress values that suggests greater resistance to erosive forces. In contrast, areas closer to the shoreline and seaward zones reveal lower τ_c values, indicating weaker, less consolidated sediments that are more vulnerable to resuspension and transport by tidal currents or wave action. This inland-to-seaward gradient in τ_c reflects the natural depositional and hydrodynamic conditions of the estuary, where seaward sediments are more frequently reworked by marine forces, resulting in finer textures and reduced cohesion. Understanding this spatial variability is crucial for assessing erosion risks.

4.2 Hydrological properties and tidal currents behavior

Water level changes in the northwestern end of the Gulf are predominantly influenced by astronomical tides, accounting for approximately 90% to 96% of variations (Lafta, 2021). The observed pattern suggests a tidal current regime characterized by semidiurnal tides, occurring twice daily.

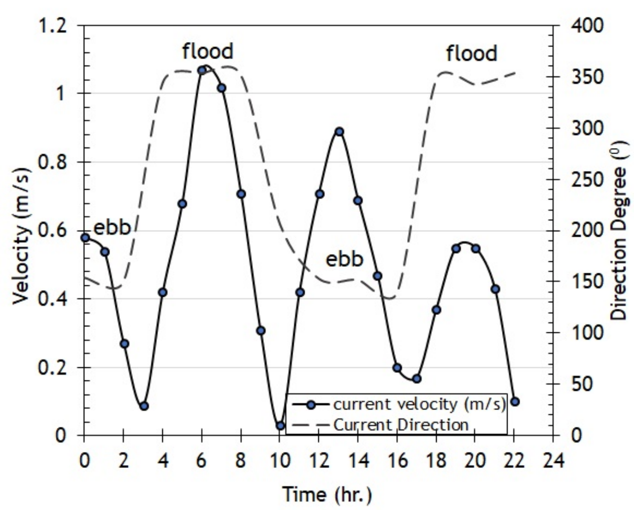

Figure 8. Speed and dircetions of tidal currents in the studty area.

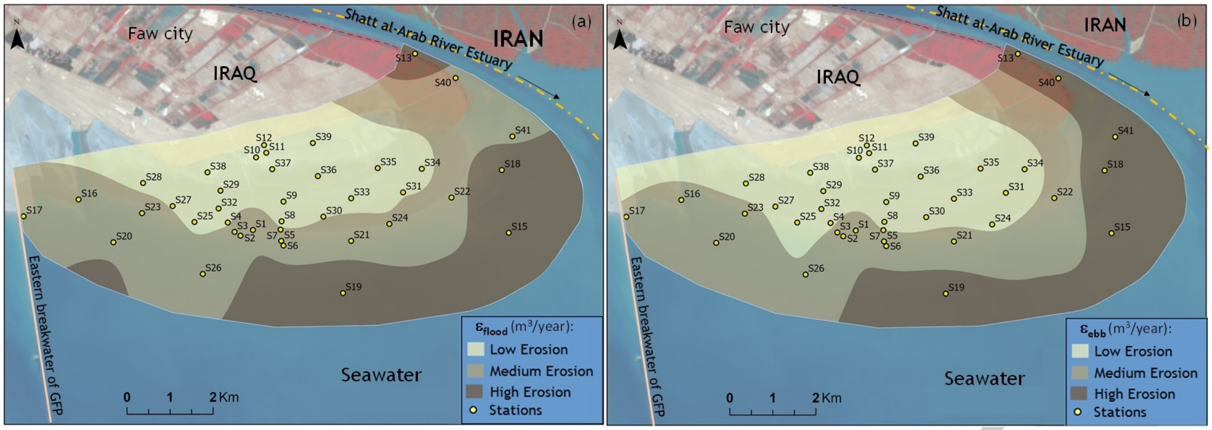

Figure 9. Erosion rates at two (a) flood (high) and (b) ebb tide conditions.

The periodic velocity peaks correspond to the flood tide, bringing water in, while the troughs correspond to ebb flows, moving water out. Figure 8 illustrates a typical pattern of the tidal currents in a study area over a 24-hour period, showing both velocity and direction of the currents. For the current velocity dynamics, it oscillates between approximately 0.05 m s^{-1} and 1.1 m s^{-1}. At the beginning, velocity starts at about 0.6 (ebb), then drops to its lowest (0.05 m s^{-1}) around hour 3. It rises sharply to a peak about (1.1 m s^{-1}) at hour 6 during the flood phase. After the peak, velocity decreases again, hitting another minimum (0.2 m s^{-1}) at hour 12 (ebb). This cycle repeats, with the second velocity peak around (0.9 m s^{-1}) at hour 15 (flood) and a smaller peak (0.6 m s^{-1}) at hour 20.

For the tidal phase, ebb is outflowing water, lower velocities, and a direction near 50°, whereas flood is inflowing water, higher velocities, and a direction near 350°.

4.3 Erosion rate analysis

The erosion rate conditions depicted in the Figure 9 illustrate the spatial variations in sediment erosion under different tidal phases, flood tide (Figure 9a) and ebb tide (Figure 9b). The study area exhibits noticeable differences in erosion intensity based on tidal influences.

The figure reveals distinct zones where high erosion rates (dark zones) dominate near the coastal front experiencing significant sediment displacement due to wave action, tidal currents, and possible anthropogenic influences such as port activity. The low erosion rates (light zones) extend further inland with less hydrodynamic process. However, as the tide recedes, Figure 8b, sediment transport mechanisms shift, resulting in lower erosion rates compared to high tide conditions (Figure 9a). Figure 9b indicates that while high erosion areas remain near the seawater side, they are less extensive than in Figure 9a. Instead, zones of moderate erosion are more widespread, suggesting gradual sediment redistribution rather than abrupt displacement. The study area experiences a general reduction in erosion intensity at ebb tide, with low erosion zones appearing along the inland portions, where water velocities weaken.

4.4 Factor of safety (FS)

Figure 10 illustrates the spatial distribution of the factor of safety (FS) under the two tidal conditions; flood tide (FS_{flood}) in Figure 10a and ebb tide (FS_{ebb}) in Figure 10b in the region. The FS values are categorized into three stability classes: stable, critical, and unstable, each indicating varying levels of geotechnical risk. In Figure 10a, the stable zones ($FS > 1.5$) are shown in dark zones, indicating areas of relative low hazard where sediments are more resistant. These regions are mostly found further inland.

In contrast, critical zones ($1.0 \leq FS \leq 1.5$) appear in, marking areas with medium hazard where sediment stability is reduced.

The unstable zones ($FS < 1.0$) are highlighted in light areas, representing high hazard areas prone to sediment instability and potential erosion or seabed failure. These areas are more heavily influenced by estuarine and tidal processes, where wave activity and tidal currents exert significant stress on the sediments.

These regions are notably concentrated in the nearshore zones adjacent to the eastern breakwater and river mouth, where dynamic tidal forces weaken sediment cohesion.

Figure 10b illustrates the FS distribution during ebb tide as tidal water levels recede. While unstable (light) zones remain, they expand slightly in area, leading to a corresponding reduction in the stable zones compared to flood tide conditions (Figure 10a). This indicates that sediment stability improves as seawater shear stress decreases. Consequently, sediment along shoreline margins experiences reduced risk during ebb tide compared to high tide.

However, unstable zones remain prominent, particularly along tidal channels and estuarine boundaries, indicating that certain regions remain geotechnically vulnerable even at ebb tide. These areas are prone to localized erosion, possibly due to residual tidal currents or sediment

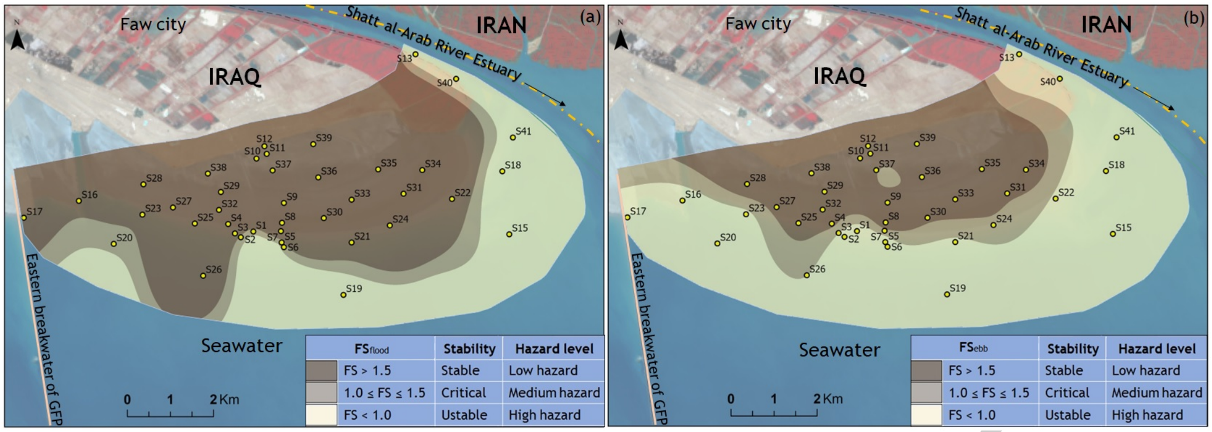

Figure 10. Hazard maps at (a) flood tide (high) and (b) ebb tide conditions according to Hadmoko et al. (2010) classification.

softening from prior tidal inundation.

5. Discussion

The integration of geotechnical and hydrological data has enabled the development of a dual-factor safety framework that captures the dynamic nature of sediment stability under alternating tidal conditions. This discussion synthesizes the key findings and interprets their implications for coastal hazard management, sediment dynamics in this vulnerable estuarine environment.

5.1 Spatial variability of sediment strength and critical shear stress

The undrained shear strength (S_u) of sediments exhibits significant spatial variability, ranging from as low as 5 kPa near the seaward edge (e.g., Station S16) to approximately 45 kPa inland (e.g., Station S10). This gradient reflects the natural depositional environment, where nearshore sediments are characterized by high water content, finer grain sizes, and lower effective stress, resulting in weaker mechanical behavior. Conversely, inland-side sediments are more compacted and cohesive due to reduced hydrodynamic disturbance and prolonged compression. The classification of S_u values into very soft, soft, and medium stiff categories based on Terzaghi et al. (1996) further supports this interpretation. The prevalence of very soft to soft sediments in the coastal front underscores the susceptibility of these zones to erosion and deformation under tidal forces.

This spatial pattern is mirrored in the distribution of critical shear stress (τ_c), which is directly derived from S_u using the empirical relationship proposed by Léonard and Richard (2004). The inland areas exhibit higher τ_c values (up to 10.5 Pa), indicating greater resistance to sediment entrainment, while the seaward zones show τ_c values below 3.0 Pa, highlighting their vulnerability to hydrodynamic forces. This inland-to-seaward gradient in τ_c is consistent with the natural sedimentological transition from consolidated clays to loosely packed, water-saturated muds.

5.2 Tidal hydrodynamics and shear stress behavior

The Ras al-Bisha region is governed by a semi-diurnal tidal regime, with two flood and two ebb tides occurring daily. The hydrological data collected from the hydrographic station near the Grand Faw Port (GFP) reveal that tidal current velocities fluctuate between 0.05 m s^{-1} and 1.1 m s^{-1}, with flood tides generally exhibiting higher velocities and more pronounced directional shifts. These alternating tidal phases exert bidirectional shear stresses on the sediment surface, necessitating a dual-factor safety approach. The applied fluid shear stress (τ_a), calculated using the equation $\tau_a = \gamma_w d S$, varies between flood and ebb conditions due to changes in water depth and slope. During flood tides, the inflowing water generates higher τ_a values, which, in many nearshore locations, exceed the critical shear stress of the sediment, leading to active erosion. Conversely, during ebb tides, the outflowing water produces lower τ_a values, resulting in reduced erosion potential. This dynamic is clearly illustrated in the erosion rate maps (Figure 9), where flood tide conditions correspond to more extensive high-erosion zones compared to ebb tide conditions.

5.3 Factor of safety and geohazard mapping

The introduction of a dual-factor safety framework, FS_{flood} and FS_{ebb}, represents a significant advancement in coastal hazard assessment. By evaluating sediment stability under both tidal conditions, the study provides a more nuanced understanding of temporal variations in geo-engineering risk. The spatial distribution of FS values reveals three distinct zones:

- Stable zones (FS > 1.5), primarily located in inland side, where sediments are more resistant to tidal forces.

- Critical zones ($1.0 \leq FS \leq 1.5$), representing transitional areas with moderate hazard potential.
- Unstable zones ($FS < 1.0$), concentrated near the shoreline and estuarine boundaries, where sediments are prone to erosion and failure.

The comparison between FS_{flood} and FS_{ebb} maps indicates that flood tides pose a greater threat to sediment stability, as evidenced by the expansion of unstable zones during high tide. However, certain areas remain geotechnically vulnerable even during ebb tides, suggesting persistent instability due to residual tidal currents, sediment softening, or anthropogenic disturbances.

The applied dual safety factor methodology transcends the traditional single-safety-factor approach by demonstrating, that the two independent safety factors, corresponding to flood (FS_flood) and ebb (FS_ebb) tidal hydrodynamic conditions, govern sediment stability and erosion hazard. This methodological advance aligns with findings from recent global studies (e.g., van Rijn, 2016; Liu et al., 2023), which encourage frameworks that account for context-specific (local) hydrodynamic variations.

5.4 Implications for coastal management and infrastructure

The findings of this study have direct implications for coastal zone management, particularly in the context of ongoing development projects such as the Grand Faw Port. The construction of the GFP has altered the coastal configuration, dividing the shoreline into morphologically distinct segments and modifying local hydrodynamics. The eastern segment, including the Ras al-Bisha zone, now experiences intensified tidal action and sediment redistribution, which may exacerbate erosion and compromise the stability of adjacent infrastructure. The identification of unstable zones near the eastern breakwater and river mouth highlights the need for targeted mitigation measures, such as sediment reinforcement, shoreline armoring, or strategic dredging. Moreover, the dual-factor safety maps can serve as decision-support tools for planners and engineers, enabling the prioritization of high-risk areas for monitoring and intervention.

5.5 Broader context and future directions

The Ras al-Bisha zone represents a microcosm of the broader challenges facing deltaic and estuarine environments worldwide. The dual-factor safety approach developed in this study offers a practical model, particularly for those experiencing rapid environmental change. Future research should explore the long-term evolution of sediment stability by developing this approach through integration of remote sensing, real-time monitoring, and machine learning to enhance predictive capabilities and support adaptive management strategies.

6. Conclusion

The engineering geological assessment of the Ras al-Bisha coastal zone demonstrates the efficacy of a dual factor of safety framework for capturing temporal variations in sediment stability under alternating tidal phases. Key findings and implications include:

- Spatial Variability of Sediment Strength: An inland-to-seaward decline in undrained shear strength (S_u: 5–45 kPa) and critical shear stress (tc: < 3–10.5 Pa) highlights the transition from consolidated clays in upland areas to soft muds nearshore towards the seaside.
- Tidal Phase Influence on Stability: Flood tides impose higher hydrodynamic stresses, expanding unstable zones ($FS_{flood} < 1.0$) close to the eastern breakwater and river mouth. Ebb tides reduce shear stress and marginally increase stable areas ($FS_{ebb} > 1.5$), though certain areas remain vulnerable.
- Geohazard Mapping as Decision Support: The dual-FS maps delineate high-risk zones for targeted interventions, such as localized armoring, sediment reinforcement, or strategic dredging, and guide port and shoreline infrastructure planning to enhance resilience against tidal erosion.
- Broader Coastal Management Considerations: The methodology offers a blueprint for other deltaic and estuarine regions where bidirectional tidal forces and human developments interact. Incorporating these findings into policy can improve sustainable shoreline management and support adaptive responses to ongoing port expansion and upstream water regulation.
- To further refine hazard predictions, future work should integrate remote sensing and real-time monitoring to track sediment dynamics under seasonal and climatic variations.

Acknowledgements

The authors acknowledge the General Company for Ports of Iraq (GCPI) and the Marine Science Center (MSC) at the University of Basrah, in Iraq for providing technical support, Data, and materials used for the study.

Conflict of interest

None declared.

References

Aladwani, N.S., 2022. *Shoreline change rate dynamics analysis and prediction of future positions using satellite* *imagery for the southern coast of Kuwait: A case study*. Oceanologia 64 (3), 417–432. https://doi.org/10.1016/j.oceano.2022.02.002

Al-Aesawi, Q.M., Al-Nasrawi, A.K., Jones, B.G., 2020. *Short-term geoinformatics evaluation in the Shatt Al-Arab Delta (Northwestern Arabian/Persian Gulf)*. J. Coast. Res. 36 (3), 498–505. https://doi.org/10.2112/JCOASTRES-D-19-00110.1

Al-Amery, A.A., Al-Saad, H.A., 2022. *Mineralogical variation of the banks of Shatt Al-Arab and Shatt Al-Basrah River sediments in southern Iraq*. Iraqi Geol. J. 55 (1A), 116–127.

Al-Asadi, S.A., Alhello, A.A., Ghalib, H.B., Muttashar, W.R., Al-Eydawi, H.T., 2023. *Seawater intrusion into Shatt Al-Arab River, Northwest Arabian/Persian Gulf*. J. Appl. Water Eng. Res. 11 (2), 289–302. https://doi.org/10.1080/23249676.2022.2113460

Albadran, B., 2004. *Shatt al-Arab Delta, Southern Iraq, sedimentological study*. Mar. Mesopotamia 1 (9), 311–322.

Albadran, B.N., Albadran, A., 1993. *Sedimentological characteristics of the offshore sediments of the Khor Abdulla entrance NW Arabian Gulf*. J. Water Resour. 2 (1), 17–34.

Albadran, N.B., Al-Manssory, F., Al-Bahily, N., 2002. *Erosion and sedimentation processes in the Shatt al-Arab*.

Alfaris, M.A., Alrubaye, A.A., Muttashar, W.R., Lo, E.L., 2024. *The compression behavior of riverine fine-grained soils treated with organic matter*. Soil Environ. 43 (2), 248–257. https://doi.org/10.25252/SE/2024/43214

Al-Fartusi, A.J., 2022. *Tidal Range and Sea Level Changes at The Area in front of Umm Qasr Port South of Iraq*. J. Univ. Anbar Pure Sci. 14 (2), 72–76. https://doi.org/10.37652/juaps.2022.172391

Al-Fartusi, A.J., Malik, M.I., Abduljabbar, H.M., 2023. *November. Spatial-temporal of Iraqi coastline changes utilizing remote sensing*. AIP Conf. Proc. 3018 (1), 020062. https://doi.org/10.1063/5.0172293

Alkhafaji, H., Muttashar, W.R., Al-Mosawi, W.M., 2023. *Proposing an inflatable rubber dam on the tidal Shatt Al-Arab River, Southern Iraq*. J. Mech. Behav. Mater. 32 (1), 20220201. https://doi.org/10.1515/jmbm-2022-0201

ASTM D2573-01, 2008. *Standard test method for field vane shear test in cohesive soil*.

ASTM D422. *Standard test method for particle-size analysis of soils*.

ASTM D4318-10, 2010. *Standard test methods for liquid limit, plastic limit, and plasticity index of soils*.

Darmoian, S.A., Lindqvist, K., 1988. *Sediments in the estuarine environment of the Tigris/Euphrates delta, Iraq, Arabian Gulf*. Geol. J. 23 (1), 15–37. https://doi.org/10.1002/gj.3350230102

Hadmoko, D.S., Lavigne, F., Sartohadi, J., Hadi, P., 2010. *Landslide hazard and risk assessment and their application in risk management and land use planning in eastern flank of Menoreh Mountains, Yogyakarta Province, Indonesia. Nat*. Hazards 54 (3), 623–642. https://doi.org/10.1007/s11069-009-9490-7

Hashemi, M., Nikoudel, M.R., Khamehchiyan, M., Hafezi Moghadas, N., 2014. *Engineering geology and geohazards of Sefidrud Delta, South Caspian Coast, North Iran*, [In:] Lollino, G., Manconi, A., Locat, J., Huang, Y., Canals Artigas, M. (eds) *Engineering Geology for Society and Territory*. Springer, Cham, 77–83. https://doi.org/10.1007/978-3-319-08660-6_16

Lafta, A.A., 2021. *Estimation of tidal excursion length along the Shatt Al-Arab estuary, southern Iraq*. Viet. J. Sci. Technol. 59 (1), 79–89. https://doi.org/10.15625/2525-2518/59/1/15433

Lafta, A.A., 2022. *Investigation of tidal asymmetry in the Shatt Al-Arab river estuary, Northwest of Arabian Gulf*. Oceanologia 64 (2), 376–386. https://doi.org/10.1016/j.oceano.2022.01.004

Lafta, A.A., 2023. *General characteristics of tidal currents in the entrance of Khor Abdullah, northwest of Arabian Gulf*. Oceanologia 65 (3), 494–502. https://doi.org/10.1016/j.oceano.2023.03.002

Léonard, J., Richard, G., 2004. *Estimation of runoff critical shear stress for soil erosion from soil shear strength*. Catena 57 (3), 233–249. https://doi.org/10.1016/j.catena.2003.11.007

Liu, X., Liu, J.P., Wang, Y.P., 2023. *Sediment dynamics and geohazards in estuaries and deltas*. Front. Earth Sci. 10, 1079804. https://doi.org/10.3389/feart.2022.1079804

Mahdi, H.A., Mahmood, R.A., Muttashar, W.R., 2025. *Iraqi shoreline stability: A review of recent geological and engineering research*. Arab. J. Geosci. 18 (6), 1–10. https://doi.org/10.1007/s12517-025-12273-7

Muttashar, W.R., Al-Aesawi, Q.M., Al-Nasrawi, A.K., Almayahi, D.S., Jones, B.G., 2024. *Coastline instability evaluation: Multitemporal bathymetric mapping and sediment characteristics*. Environ. Earth Sci. 83 (1), 43. https://doi.org/10.1007/s12665-023-11375-3

Muttashar, W.R., Al-Whaely, U.Q., Almayahi, D.S., Hussein, M.A., Al-Aesawi, Q.M., Lafta, A.A., Chassib, S.K., 2025. *Quantifying the level of erosion-induced hazards on tidal riverbanks*. Nat. Hazards Res. 5 (3), 678–688. https://doi.org/10.1016/j.nhres.2025.02.007

Muttashar, W.R., Bryson, L.S., Al-Humaidan, Z.A., 2021. *The use of particle size distribution integrated with consistency limits for experimentally simulating fine-grained sedimentary units*. Arab. J. Geosci. 14, 1–12. https://doi.org/10.1007/s12517-021-08812-7

Sun, H., Zhao, Z., Ruan, X., Chu, Y., Fan, C., 2025. *Large-scale evaluation of beach morphodynamic evolution and environmental drivers along China's eastern coast through long-term Landsat analysis*. Earth's Future 13 (9), e2025EF006058.

https://doi.org/10.1029/2025EF006058

Terzaghi, K., Peck, R.B., Mesri, G., 1996. *Soil mechanics in engineering practice*, 3rd edn. Wiley, New York, 549 pp.

van Rijn, L.C., 2016. *Stability design of coastal structures (seadikes, revetments, break-waters and groins)*.